



<http://www.diva-portal.org>

## Postprint

This is the accepted version of a paper published in *Journal of Renewable and Sustainable Energy*. This paper has been peer-reviewed but does not include the final publisher proof-corrections or journal pagination.

Citation for the original published paper (version of record):

Göteman, M., Engström, J., Eriksson, M., Isberg, J., Leijon, M. (2014)

Methods of reducing power fluctuations in wave energy parks.

*Journal of Renewable and Sustainable Energy*, 6: 043103

<http://dx.doi.org/10.1063/1.4889880>

Access to the published version may require subscription.

N.B. When citing this work, cite the original published paper.

Permanent link to this version:

<http://urn.kb.se/resolve?urn=urn:nbn:se:uu:diva-233752>

# Methods of reducing power fluctuations in wave energy parks

Malin Göteman,<sup>a)</sup> Jens Engström, Mikael Eriksson, Jan Isberg, and Mats Leijon

*Department of Engineering Sciences, Division of Electricity, Uppsala University, Box 534, SE-751 21 Uppsala, Sweden*

(Dated: 29 April 2014)

One of the major challenges in constructing effective and economically viable wave energy parks is to reduce the large fluctuations in power output. In this paper, we study different methods of reducing the fluctuations and improve the output power quality. The parameters studied include the number of devices, the separating distance between units, the global and local geometry of the array, sea state and incoming wave direction, and the impact of including buoys of different radii in an array. Our results show that, e.g., the fluctuations as well as power per device decrease strictly with the number of interacting units, when the separating distance is kept constant. However, including more devices in a park with fixed area will not necessarily result in lowered power fluctuations. We also show that varying the distance between units affects the power fluctuations to a much larger extent than it affects the magnitude of the absorbed power. The fluctuations are slightly lower in more realistic, randomized geometries where the buoys tend to drift slightly off their mean positions, and significantly lower in semi-circular geometries as opposed to rectangular geometries.

Keywords: wave energy, WEC arrays, hydrodynamics

## I. INTRODUCTION

The energy absorption of a single point-absorbing wave energy converter (WEC) is limited; to produce a power of more than a few MW, enable an even power distribution and construct cost effective wave energy solutions, future designs of wave energy will necessarily involve large arrays of many absorbing units. These individual devices will interact both hydrodynamically and electrically, which raises new questions regarding performance and design of the wave energy parks. The problem of reducing fluctuations in wave power parks was considered already in early works on wave energy<sup>1,2</sup> and has received new attention recently, when wave energy is taking the step into full-scale commercial farms. Papers of particular interest for this paper that are treating fluctuations include<sup>3-9</sup>.

Many parameters might affect the performance: the number of devices, the separation between units, the characteristic dimensions of the WECs, geometry of the park, wave climate and incoming wave direction, control strategies, mooring configurations, etc. To find optimized solutions for wave energy parks, all these parameters deserve detailed studies in their own respect. In this paper, we study a few of the mentioned parameters and try to give a coherent overall picture and provide guidelines relevant for the planning of wave energy parks, with focus on lowering the power fluctuations. The interaction by radiated and scattered waves between all devices in the park are computed using the boundary element potential flow solver WAMIT, and the hydrodynamical coefficients are used as input in a time-domain model to simulate the dynamics and power of the WECs and the park.

## II. THEORY

### A. Linear potential flow theory

In this paper, we consider WECs of point-absorber type with a semi-submerged buoy at the sea surface connected via a line to a direct-driven linear generator at the seabed, described more in detail in section III A. The water domain has finite depth  $h$  and density of water  $\rho$ . The buoy is modelled as a solid cylinder with radius  $R$  and draft  $d$ , and is restricted to move in heave only. The coordinate system is chosen such that  $z = -h$  at the seabed,  $z = -d$  at the bottom of the cylinder buoy when not oscillating, and  $z = 0$  at the undisturbed sea surface.

The equation of motion for each heaving cylinder is given by Newtons second law; the oscillatory motion is excited by the incoming waves and damped by the radiated waves from the own oscillations, from the static restoring force for submerged bodies and from the power take-off,

$$m\ddot{z}(t) = F_{\text{exc}}(t) + F_{\text{rad}}(t) + F_{\text{stat}}(t) + F_{\text{PTO}}(t), \quad (1)$$

where  $z$  is the vertical coordinate of the buoy. The hydrostatic force is Archimedes' principle of restoring force on submerged bodies,  $F_{\text{stat}}(t) = -\rho g \pi R^2 z(t)$ , and the power take-off force is modelled as a linear damping and spring force,  $F_{\text{PTO}} = -\gamma \dot{z}(t) - k_s z(t)$ . The excitation force and radiation force are dynamical and given by the pressure integrated along the wetted surface of the buoy. Under the assumption of a homogeneous, non-compressible, ideal, irrotational fluid, the fluid potential satisfies the Laplace equation  $\Delta\Phi = 0$ . In this paper we assume non-steep waves, implying that the non-linear boundary conditions at the free sea surface can be linearised and the first-order linear approximation taken.

The hydrodynamical coefficients will be calculated in the frequency domain, and the physical observables are

---

<sup>a)</sup> malin.goteman@angstrom.uu.se

given by the inverse Fourier transforms. In the linearised potential flow theory, the total wave potential can be decomposed into potentials for the incoming waves  $\phi_{\text{in}}$ , scattered waves  $\phi_S$  and radiated waves  $\phi_R$  from the oscillations of the body,  $\phi = \phi_{\text{in}} + \phi_S + \phi_R$ . The dynamical force on the cylinder of the waves is given by the pressure integrated along the wetted surface of the buoy, which in the frequency domain is proportional to the wave potentials. The force resulting from the incoming and scattered waves is the excitation force factor  $f_{\text{exc}}(\omega)$ ; the force originating from the radiated waves is the radiated force, with real and imaginary parts proportional to the added mass  $m_{\text{add}}(\omega)$  and the radiation damping coefficients  $B(\omega)$ , respectively. In the frequency domain, the dynamical equation in (1) can be solved for the vertical coordinate  $z(\omega)$  as

$$z(\omega) = \frac{f_{\text{exc}}(\omega) \eta_{\text{in}}(\omega)}{\rho g \pi R^2 + k_s - (m + m_{\text{add}}(\omega)) \omega^2 - i(B(\omega) + \gamma) \omega}, \quad (2)$$

or  $z(\omega) = H(\omega) \eta_{\text{in}}(\omega)$ , where  $H(\omega)$  is the transfer function (response amplitude operator) and  $m = m_t + \rho \pi R^2 d$  the total mass of the translator and the submerged buoy. The vertical position of the buoy is then obtained in the time-domain by inverse Fourier transform. With the position of the buoy in time determined, the absorbed power of the WEC can be calculated as  $P(t) = \gamma \dot{z}(t)^2$ . The performance of a WEC is usually measured in terms of a power capture ratio (PCR) between the time-averaged power absorption and the incident energy transport over the buoy diameter,  $\text{PCR} = \bar{P}/(2RJ)$ , where the incident energy transport for waves in waters of infinite depth can be defined as  $J = (\rho g^2/64\pi) T_e H_s^2$ . The energy period  $T_e$  and the significant wave height  $H_s$  characterize the sea state and are defined in terms of spectral moments.

## B. Interacting units in a wave energy park

Consider a system of  $N$  WECs, each with a generator at the seabed connected to a floating buoy with vertical position  $z_j(t)$  with index  $j \in [1, N]$ . All the buoys will interact by scattered and radiated waves. The dynamics of each buoy is calculated from a system of coupled equations of motion according to the procedure described above, with the transfer functions  $H_j(\omega)$  and hydrodynamical coefficients calculated individually.

The park effect can be represented as the ratio of the power of the full array divided by the sum of the power of each isolated WEC<sup>10</sup>

$$Q = \frac{P_{\text{tot}}}{\sum_{j=1}^N P_j^{(\text{isolated})}}. \quad (3)$$

Although certain park configurations may have constructive interaction, where  $Q > 1$  and the average power per WEC is larger than for isolated WECs, in realistic scenarios with irregular waves and many interacting units,

the interactions are destructive<sup>11</sup>, and measures must be taken to minimize the destructive interactions. In particular, it is shown that the park effect factor in (3) integrated over all incoming wave directions equals one<sup>12,13</sup>, in other words, if a certain wave park configuration is optimal with  $Q > 1$  in one incoming wave direction, then there are necessarily other wave directions for which the layout is not favourable. This is of relevance when discussing some of the park geometries described in the next section, that are sensitive to the wave direction and optimal in certain directions, but not in others.

## C. Variance

As described in the introductory section, one of the most important effects of park interactions are the reduction of power fluctuations. The fluctuations in a park with  $N$  WECs can be measured in terms of the normalized variance of the total array power, which is defined in terms of the standard deviation as  $v = \sigma^2(P_{\text{tot}})/\bar{P}_{\text{tot}}^2$ .

## III. METHOD

### A. Model specification

The physical parameters used in the simulations are based on the wave energy converter developed at Uppsala University. The WEC is of point-absorber type, with a semi-submerged buoy at the sea surface connected to a direct-driven linear generator at the seabed<sup>14</sup>. The characteristic dimensions of the WECs and the wave climate used in the simulations are given by table I. Three different buoy radii, ranging from 1.5 m to 3.5 m, and corresponding damping coefficients are considered. The constant damping coefficients are chosen to give optimal power absorption for the given buoy size for one sea state measured during 30 minutes at the west coast of Sweden. The chosen sea state is characterized by energy period  $T_e = 5.01$  s and significant wave height  $H_s = 1.53$  m and lies within the range of the most common sea states at the test site location. In arrays where only one size of buoys are considered, the radius  $R_2 = 2$  m and corresponding damping coefficient  $\gamma_2 = 55\,000$  Ns/m are used.

The Uppsala University WECs are deployed at a full-scale research site at Lysekil, at the west coast of Sweden. At this test site, 44% of the annual energy flux occurs for sea states characterized by an energy period  $T_e$  in the interval 4-7 s and a significant wave height  $H_s$  in the interval 1-3 m<sup>15</sup>. Variations in the water level due to tides and air pressure variations are very small and have been neglected in this paper. The sea states used in this study are measured time series of uni-directional, irregular wave elevation data collected at the research site. The data is obtained by a non-directional Datawell Waverider buoy at a sampling rate of 2.56 Hz. In total, 10 sea states

TABLE I. Characteristic dimensions of the WECs and the energy periods  $T_e$  and significant wave heights  $H_s$  of the sea states used. Sea state number 5 is used in all simulations where only one sea state is considered.

<i>WEC characteristics:</i>		<i>Sea states:</i>		
		#	$T_e$ [s]	$H_s$ [m]
Buoy radius [m]	$R_1 = 1.5$	1	4.68	1.13
	$R_2 = 2.0$	2	4.85	1.31
	$R_3 = 3.5$	3	4.86	0.82
Buoy draft [m]	$d = 0.5$	4	4.86	1.14
Translator mass [kg]	$m_t = 2560$	5	5.01	1.53
Spring constant [N/s]	$k_s = 4000$	6	5.47	1.03
Damping coefficient [Ns/m]	$\gamma_1 = 41000$	7	5.61	1.13
	$\gamma_2 = 55000$	8	5.76	1.03
	$\gamma_3 = 200000$	9	6.25	2.37
		10	7.34	2.36

are considered; their energy period and significant wave height are described in table I.

As explained in section II A, the dynamical parameters in the equations of motion for the buoy are the exciting force, the added mass and the radiation damping. The hydrodynamical coefficients are computed using WAMIT, and used as inputs in a time-domain model in Matlab, where the dynamics of the WECs and the absorbed power are calculated as described in section II.

## B. Parameters affecting variance and power output

Many parameters in a wave energy park may influence variance of power output. Several of these have been subject to previous studies, and also summarized in review papers<sup>8</sup>. In this paper, we study and compare the impacts of varying a few of the different parameters, and try to give a coherent picture and provide guidelines relevant from an engineering perspective on wave park design. In this section, we review earlier results on the subject, and motivate and describe the outline of our study.

### 1. Number of devices

A number of papers have studied the effect of adding more devices to an array. In<sup>16</sup>, square arrays of  $4 \times 4$  and  $5 \times 5$  oscillating surge converters (OWSC) were studied, and the conclusion was drawn that the absorbed power of the row  $n$  furthest from the incoming wave can be approximated by the power of the previous row as  $P_n \sim QP_{n-1}$ , where  $Q$  is defined in equation (3). In<sup>5</sup>, experimental data from 3 WECs show that the variance reduces with increased amount of buoys (2 and 3 buoys as compared to one single buoy), with increased damping and with significant wave height. Similarly, simulations of 5 and 10 buoys are used to argue that the power fluctuations decrease with increased amount of buoys in<sup>3</sup>. In<sup>17</sup>, results

of experiments with 24 WECs in an array were compared with simulations. It was seen from experiments that up to 26% of the energy yield from an equivalent number of isolated WECs may be lost due to interference effects. Using a point-absorber approximation for simulations of up to 30 SEAREV devices in a double half circle, the variance of the power was shown to decrease with increased number of devices, and the statement that it is unrealistic to achieve a standard deviation of less than 20% was postulated<sup>4</sup>. In<sup>7</sup>, the power variance was studied for parks with 1, 5, 6, 10 and 12 WECs in different configurations, and was found to be reduced from 1.41, 0.99, 0.84, 0.47 and 0.66, showing that the variance depends on the number of devices but also on the geometry.

In<sup>9</sup>, we studied semi-circular arrays with 12, 22 and 32 WECs, and compared them with isolated single WECs. For the same wave climate, the variance was reduced from roughly 2 for an isolated WEC to 0.30, 0.26 and 0.24 for 12, 22 and 32 WECs, respectively. Here, we study the variation as a function of the number of WECs in more detail, and include arrays ranging from 4 to 64 devices. The results are presented in section IV A.

### 2. Spacing between devices

Earlier studies have indicated that the park effect can be neglected at large separating distances. In<sup>18</sup>, it was shown that the performance is independent of the spacing for separating distances greater than  $4R$  (where the radius ranges between  $2.5 < R < 10\text{m}$ ). Similarly, a system of two heaving WECs was found to have negligible interactions when the separation distance is a few hundred meters<sup>19</sup>, and lower than 5% for separation distances larger than 100 m<sup>16</sup>. However, to minimize the used ocean area and cost of sea cable, commercial wave parks will most likely be forced to deploy devices in close proximity. Hence, the effects of the spacing between devices must be studied thoroughly to optimize the design of wave farms.

In<sup>4</sup>, the normalized standard deviation of power was plotted as a function of distance between SEAREV devices. However, the deviations found did not exceed 10% and were within the range of noise on the results. Here, we study arrays with nine devices with varying distance between adjacent buoys, and find that the variance does depend on the distance, as described in section IV B.

### 3. Park geometry

*a. Global park geometry* The global geometry can have a large effect on the output power and the fluctuations in an array. In<sup>20</sup>, it was shown that certain array layouts can increase the power with 5% or lead to a decrease of up to 30%. In<sup>17</sup>, three different configurations of arrays with 24 WECs were compared in experiments and simulations. The proportional increase in yield from

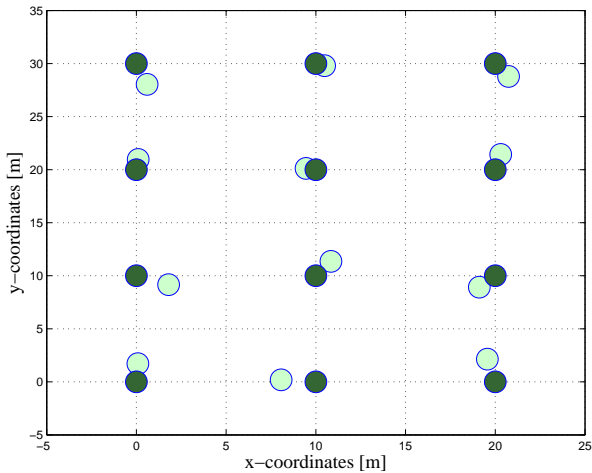


FIG. 1. Difference between regular and randomized geometries; the darker units have exact positions on the lattice, whereas the pale units are slightly randomized, as is the case when floating buoys drift slightly off their mean positions.

the worst to best layout was found to be as high as 28%. Several park configurations for small arrays of up to 12 WECs were compared in<sup>7</sup>, and it was shown that some park geometries have positive interference factor.

In<sup>21</sup> and<sup>22</sup>, arrays with WECs in  $45^\circ$  angle to the incoming wave direction were found to be optimal to gain power quality from intermediate power smoothing, while simultaneously achieve good capture ratio, which requires spacing perpendicular to the incoming wave direction. The geometry was further explored in<sup>6</sup>, where six arrays, each consisting of 7 WECs arranged in  $45^\circ$  angle to the incoming wave, were combined in a wedge-shaped park of  $6 \times 7$  WECs. The peak-to-average power ratio was in this array geometry reduced to 1.56. Half-circular double arrays were considered in<sup>4</sup> and compared to arrays with WECs in diamond shaped lattices. Under the point-absorber assumption, no difference on the variance was found between these two layouts.

In<sup>9</sup>, we compared arrays of 32 WECs in rectangular and semi-circular configurations. Whereas the rectangular geometry reduced the power variance of single isolated WECs to 0.45-1.15 (depending on wave climate), the circular geometry displayed a variance as low as 0.15-0.40.

In this paper, we study rectangular and semi-circular geometries, with a particular focus on rectangular ones.

*b. Local park geometry* Not only the global geometry of the array is relevant for the power fluctuations. In realistic scenarios, the positions of the buoys will not be exact on grid vertices, but instead tend to drift slightly off their mean positions, see figure 1. In a previous paper<sup>9</sup>, we included this observation and studied each geometry also in a slightly randomized setting. In all global geometries, the variance was found to be reduced in the (more realistic) randomized version. The difference between the randomized and regular geometries was more profound for rectangular global geometries than for semi-circular

global geometries, where the variance was already low.

*c. Incoming wave directions* Using point-absorber approximation in<sup>12</sup>, and later full linear interactions in<sup>13</sup>, the interaction factor in (3) was shown to be equal to one when integrated over all incident wave directions. This implies that if a certain park configuration has incoming wave angles for which the interaction factor is constructive, i.e. the total power obtained is higher than the sum of the single isolated WECs, then there are necessarily other unfavourable wave angles where the interaction is destructive. Several authors have studied the park effect for different configurations; e.g.,<sup>20</sup> who found optimal configurations where the interaction factor was maximized, and<sup>7</sup> who compared different incident wave angles and observed a less positive interference when the wave propagates along the aligned array direction, which represents a shadowing effect. However, as pointed out in<sup>11</sup> and recently in<sup>8</sup>, in realistic scenarios, the interaction factor will be destructive, and array layouts should be optimized to minimize destructive interactions.

However, wave angles that maximize the power might not be optimal for minimizing the fluctuations, and studies must include both aspects to find optimal design guidelines for full-scale wave power parks. In<sup>21</sup>, a linear row of WECs was considered and the peak-to-average power ratio was seen to be reduced as a function of incoming wave angle perpendicular to the row. Optimal incoming wave angle with regard to both power smoothing and good capture ratio was found to be  $45^\circ$ <sup>22</sup>. A disparate result was obtained in<sup>4</sup>, where the conclusion was drawn that the fluctuations do not depend strongly on the directionality of the waves.

Here, we study the performance of a specific array consisting of buoys of different radii as a function of incoming wave angle. The results are presented in section IV C.

#### 4. Sea state

Obviously, the sea state has a large impact on the performance of a WEC; the dynamics of the buoy is calculated as a convolution with the wave amplitude as described in section II A, and sea states with comparable energy period but higher significant wave height give larger power output.

The impact of the sea state on the power fluctuations is less studied. Some studies have indicated that the magnitude of the fluctuations is not related to the sea state conditions<sup>4</sup>, and the three sea states studied in<sup>21</sup> displayed a similar peak-to-average power ratio as a function of angle. In<sup>9</sup>, we compared power and variance for 34 sea states and found a large scattering for the variance as a function of energy period. In this paper, we find that the sea states show different behaviour as function of the separating distance, as described in section IV D.

## 5. Size of buoys

The effect of mixing sizes of the buoys in an array has, to the authors' knowledge, not been presented before. In this paper, we study and compare arrays with nine buoys of three different sizes, see figures 2-3 for rectangular and semi-circular geometries, respectively. Extreme cases are given by configurations where the buoy sizes are strictly increasing or decreasing along the wave direction; geometry 4 and 6 in figure 2 (which corresponds to incoming angle  $\chi = 0^\circ$  and  $\chi = 180^\circ$  for the same park) and geometry 12-13 in figure 3. The results of the comparisons are presented in section IV E.

## IV. RESULTS

### A. Number of devices

In figure 4, the results for the variance and power per WEC are plotted as functions of the number of WECs in rectangular array geometries. The distance between adjacent buoys is 10 m in the regular park configurations, and approximately the same in the randomized geometries. The incoming angle is  $\chi = 0^\circ$  and the sea state used has energy period  $T_e = 5.01$  s and significant wave height  $H_s = 1.53$  m.

In the case of non-square, rectangular arrays (e.g.,  $2 \times 3$  and  $3 \times 2$  WECs), different configurations are possible and have different properties. To make a fair comparison of arrays with different number of WECs, we include both the most and least favourable geometry from the point of view of lowering the variance. E.g., for an array with 12 WECs we include both the configurations  $4 \times 3$  and  $3 \times 4$  WECs along the wave direction. The two configurations are compared in table II and a mean of the configurations are plotted in figure 4.

The variance reduces drastically with the number of interacting WECs, from 0.91 in an array with four WECs to 0.41 in an array with 64 WECs, as shown in figure 4. Also the time-averaged power per WEC reduces, from 6 kW per WEC in the array with four WECs to 4.4 kW in the array with 64 WECs.

As will be discussed in section IV B, the power variance in a park also depends on the distance between adjacent WECs. To eliminate this factor, the simulations plotted in figure 4 consider parks with constant separation distance of 10 m between the WECs. However, for engineering purposes, it might be relevant to consider parks of constant areas, but to increase or decrease the number of WECs within the given area. To study this parameter, we have also performed simulations of parks with equal area  $70 \times 70$  m<sup>2</sup> but different number of buoys, varying from  $2 \times 2 = 4$  to  $8 \times 8 = 64$  WECs. The result is plotted with crosses in the same figure 4. Also in this case, the power per WEC reduces as a function of the number of buoys. However, due to the fact that the interactions between the devices depend on the distance

between them, the corresponding variance does not follow a strict decrease. For example, the variance in the park with 9 WECs ( $3 \times 3$  separated by distances of 35 m) is 0.61 and lower than in the park with 16 WECs ( $4 \times 4$  separated by distances of 23.3 m), where the variance is 0.76. Hence, the power variance in a wave energy park is not automatically lowered when the number of buoys is increased; careful investigation of the separating distance must be performed.

### B. Spacing between devices

As seen in the previous section, the variance and power per WEC are strictly decreasing with the number of WECs in an array, when the separating distance between two adjacent units is kept constant, but not if the distance is allowed to vary. In this section, we investigate the variance and power per WEC as a function of distance between WECs in more detail. Square arrays of  $3 \times 3$  with separating distances between two devices ranging from 5 m to 79 m are studied, and nine different sea states are compared. The results are presented in the figures 5-6.

In figure 5, three sea states with comparable energy period  $T_e \sim 4.86$  s and significant wave heights ranging from  $H_s = 0.82$  m to  $H_s = 1.31$  m are compared. As expected, the power increases with the wave height, when the energy period is kept constant. We see that the park effect, i.e. that the total power of the array differs from the sum of the individual isolated WECs, is most important for separating distances less than 10 m. For larger distances, the average power per buoy is more or less constant.

As a contrast, the power variance depends strongly on the distance between the devices, and fluctuates also for larger separations. For all three wave climates, the variance has peaks at distance  $\sim 20$  m and local minimas at distances 10 m and 35 m. The oscillatory pattern of the variance is less significant for separating distances larger than 40 m.

The results in figure 6 are based on simulations for six different wave climates and displayed in pairs of two sea states with comparable significant wave heights, but differing energy periods. In the first case, the significant wave height is relatively low,  $H_s = 1.03$  m, and the energy period differs only by 0.3 s. As a result, the two sea states have comparable average power per WEC. The variance however, differs, and except for the local minima at 10-15 m, the oscillatory patterns are less visible and not in phase. The second and third cases consider sea states with significant wave height  $H_s = 1.13$  m and  $H_s \sim 2.37$  m, respectively. In both cases, the energy period differs by about 1 s, with the result that the power output is slightly higher in the case with shorter period. The oscillatory pattern of the variance as a function of the separating distance between units is more visible in some of the sea states.

Hence, in a park with 9 WECs in a square array, the

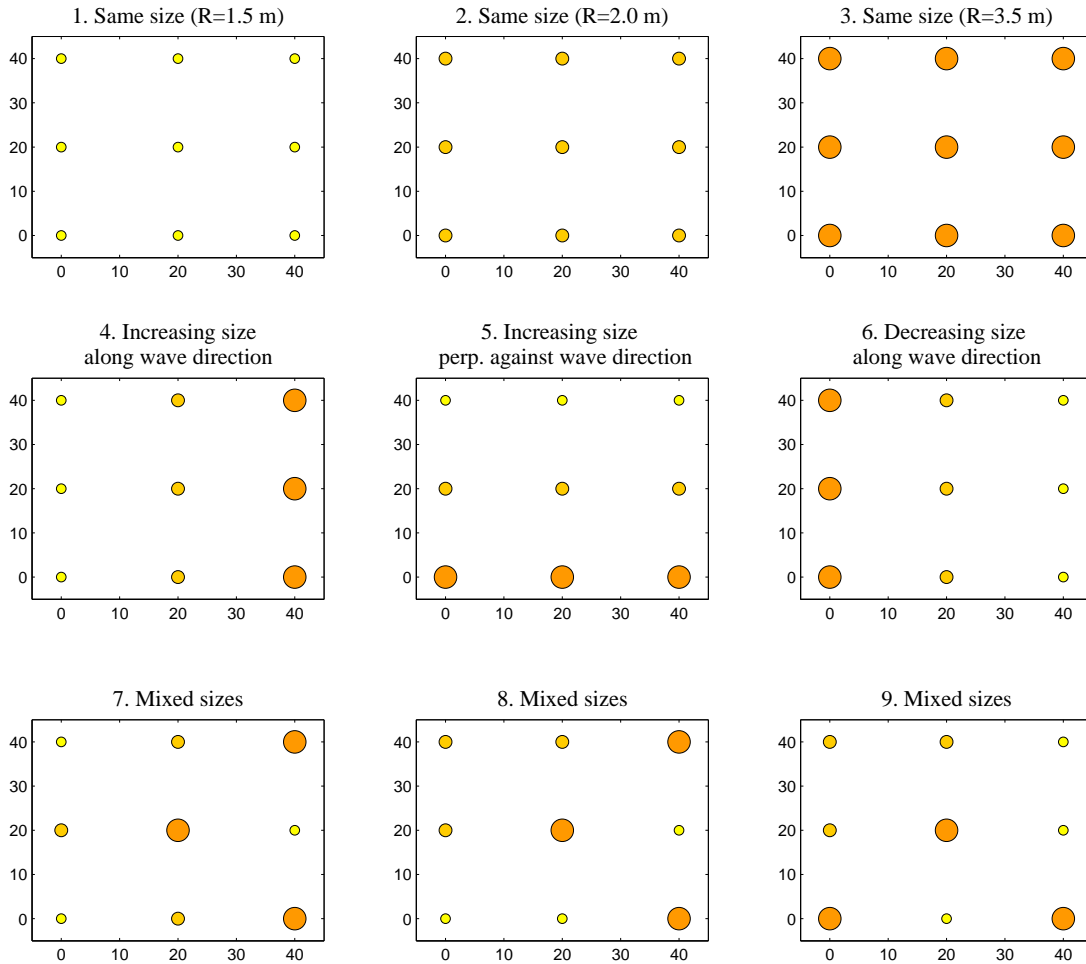


FIG. 2. Small parks with 9 WECs and buoys of different radii. The  $x$ - and  $y$ -axes are given in [m] and the incoming wave direction is  $\chi = 0^\circ$  along the  $x$ -axis. Geometry 1-3: radius  $R_1 = 1.5$  m,  $R_2 = 2.0$  m,  $R_3 = 3.5$  m in the arrays, respectively. Geometry 4-5: radius increases from  $R_1$  to  $R_3$  along, perpendicular or against the wave direction. This geometry will be studied separately as a function of incoming wave direction, but these three extreme configurations, corresponding to incoming wave angles  $\chi = 0^\circ$ ,  $\chi = 90^\circ$  and  $\chi = 180^\circ$ , are included here for comparison. Geometry 7-9: Mixed sizes as seen in the figure.

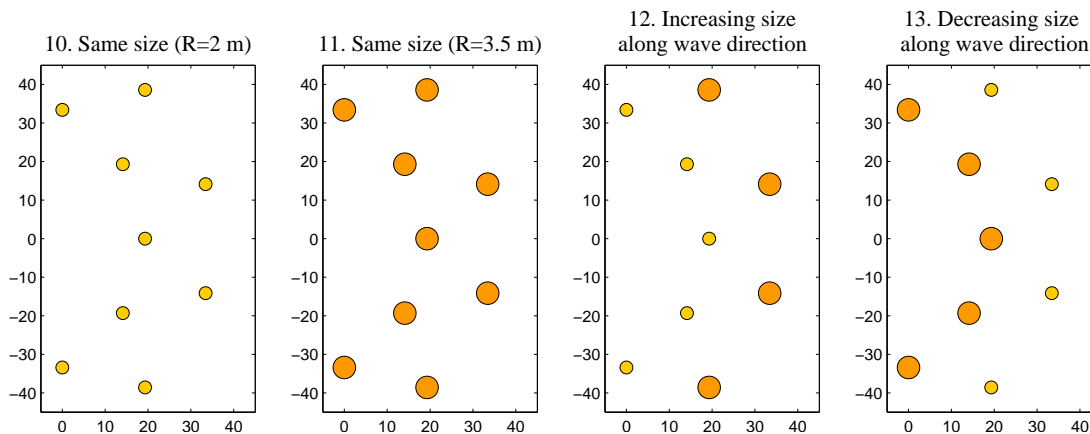


FIG. 3. Small semi-circular parks with 9 WECs and different sizes of buoys. The  $x$ - and  $y$ -axes are given in [m] and the incoming wave direction is  $\chi = 0^\circ$  along the  $x$ -axis. Geometry 10-11: radius  $R_2 = 2.0$  m and  $R_3 = 3.5$  m in the arrays, respectively. Geometry 12-13: radius increases from  $R_2$  to  $R_3$  along and against the wave direction, respectively.

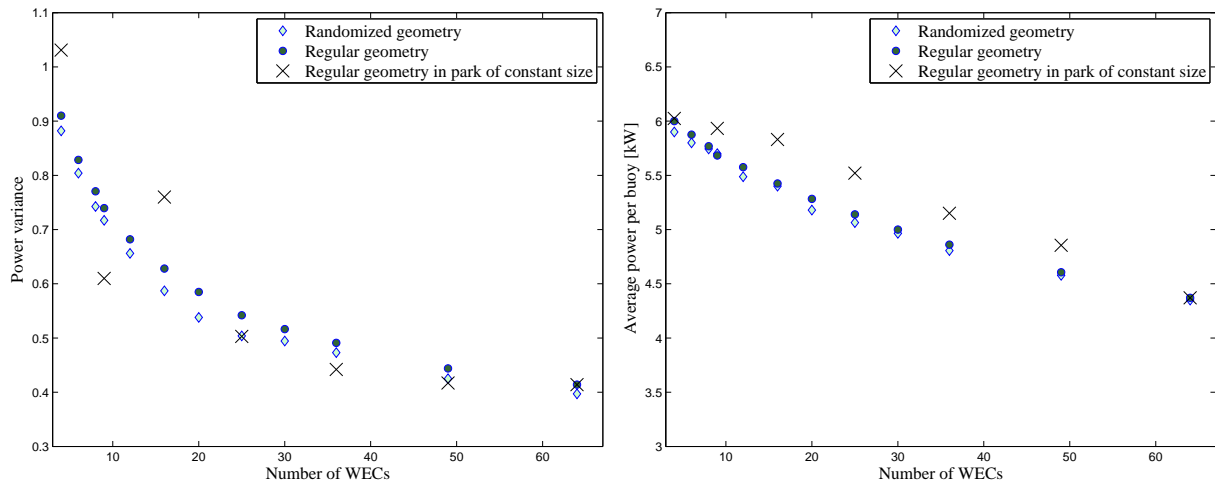


FIG. 4. Variance and corresponding time-averaged power per WEC as a function of units in the wave energy park. The dark blue circles correspond to the regular geometry, where the WECs have exact positions on the lattice, whereas the pale diamonds correspond to slightly randomized geometries, as pictured in figure 1. The crosses correspond to square arrays of 4, 9, 16, 25, 36, 49 and 64 WECs in an area of  $70 \times 70 \text{ m}^2$ .

variance displays an oscillatory pattern as a function of the separating distance between adjacent units. In all compared sea states, a local minima is obtained at 10-15 m and peaks at 20-35 m. Expressed differently, in all investigated sea states, a square park occupying an area of  $400 \text{ m}^2$  (separating distance 10 m) has considerably lower variance than a park occupying an area of  $1600 \text{ m}^2$  (separating distance 20 m).

### C. Park geometry

#### 1. Global geometry

In this paper, most focus is put on comparing rectangular arrays, but a small semi-circular configuration is included for comparison, see figure 3. The separating distance between adjacent units in the semi-circular configurations (geometry 10-13) is about 20 m and comparable to the separating distance in the square arrays displayed in figure 2 (geometry 1-9). The variance and total power of the array are plotted for each geometry in figure 7. In particular, the rectangular geometry number 2 and the semi-circular geometry 10 both consist of 9 WECs with buoy radius  $R_2 = 2 \text{ m}$  and are comparable. The power per WEC is comparable for the two arrays, but the variance differs substantially: 0.68 for the semi-circular and 0.87 for the rectangular array. Equivalent results are obtained when comparing geometry 3 and 11, both being arrays with 9 WECs of the same buoy size  $R_3 = 3.5 \text{ m}$  in rectangular and semi-circular geometry, respectively. Again, the time-averaged power for the two parks are comparable, albeit slightly higher in the semi-circular array (120.5 kW as compared to 112.9 kW in the rectangular array), but the variance is significantly

TABLE II. Comparison of the variance and average power per WEC in kW between the most and least favourable configurations of non-square, rectangular arrays, as described in section III. The incoming wave is along the x-axis; hence  $N_x$  and  $N_y$  are the number of rows along and perpendicular to the wave direction, respectively. The mean values of the two configurations are plotted in figure 4.

$N$	$N_x \times N_y$	variance	$\bar{P}_{\text{WEC}}$	$N_x \times N_y$	variance	$\bar{P}_{\text{WEC}}$
6	$2 \times 3$	0.92	6.1	$3 \times 2$	0.74	5.7
8	$2 \times 4$	0.92	6.2	$4 \times 2$	0.62	5.4
12	$3 \times 4$	0.74	5.8	$4 \times 3$	0.63	5.4
20	$4 \times 5$	0.63	5.5	$5 \times 4$	0.54	5.1
30	$5 \times 6$	0.54	5.2	$6 \times 5$	0.49	4.8

lower; 0.73 as compared to 0.89 in the rectangular array. Hence, we can see that the semi-circular geometries have lower variance than the square arrays, which supports the earlier findings in<sup>9</sup> and other references discussed earlier.

Regarding the non-square, rectangular geometries of different sizes, different properties for the variance and power are obtained if the rows and columns are interchanged, as discussed earlier. For example, a park of  $4 \times 5 = 20$  WECs has lower variance if there are 5 rows along the direction of the wave, as compared to 4. (Which can, of course, equally well be described in terms of wave direction  $0^\circ$  and  $90^\circ$  degrees.) The most and least favourable configurations are compared in table II, and a mean over them are plotted in figure 4. From table II, it is clear that the the number of rows  $N_x$  along the wave direction govern the properties to a larger extent than the number of rows perpendicular to the wave direction; increasing rows  $N_x$  from 2, 3, 4 to 5 reduces the variance from 0.92, 0.74, 0.63 to 0.54, independent of the total number of WECs.

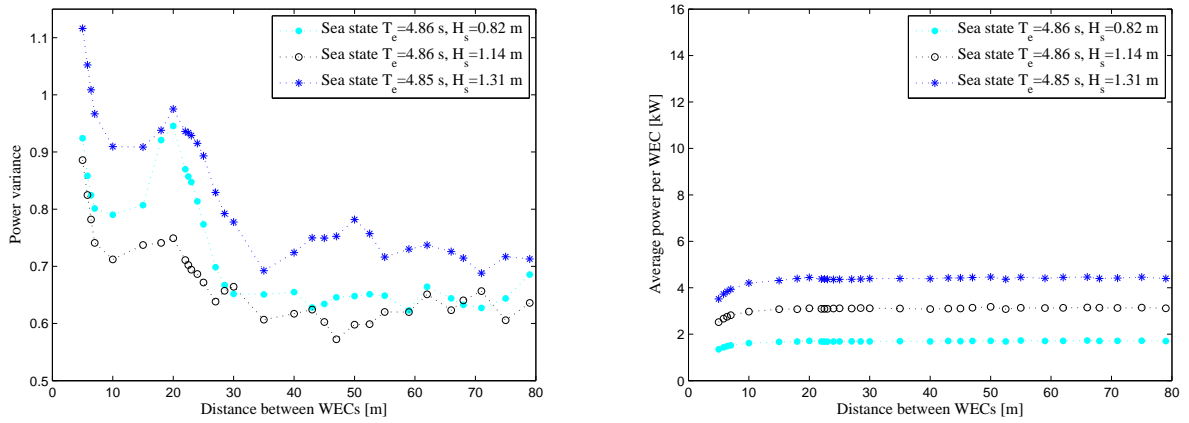


FIG. 5. Power variance and average power per buoy as functions of distance between adjacent devices in a wave energy park with 9 WECs. Three different sea states with comparable energy period but differing significant wave height are compared regarding variance and average power per WEC. The dotted lines are included only as a guidance for the eye.

## 2. Local geometry

In realistic situations, the positions of the buoys will not be exact, but instead tend to drift slightly off their mean positions. This local geometry affects the power variance of the park. Figure 4 compares simulations of regular arrays with arrays of slightly randomized geometries. In the simulations of the rectangular arrays in figure 4, the variance of the randomized arrays are between 92-97% of the regular ones. Also the power per WEC is slightly lower for the randomized geometries, but the difference is not as significant.

## 3. Incoming wave direction

As described in section II, if the interaction factor (3) is larger than one for one incoming wave direction, then the interaction effects are necessarily destructive in other wave directions. Similarly, here we will see that certain configurations are favourable in some wave directions, but unfavourable in others. As discussed above, several of the different array configurations discussed in this paper can be regarded as the same with different incoming wave angles. For example, this is true for the geometries 4-6 in figure 2 and in the non-square, rectangular configurations displayed in table II, where it was clear that increasing number of rows along the wave direction reduces the power fluctuations.

To study the properties of the wave park as function of the wave direction in more detail, a sweep over the incoming wave directions  $0^\circ$  to  $360^\circ$  was performed for geometry 4(-6). As seen in figure 8, the power is maximized when the buoy sizes increase along the wave direction, and minimized in the opposite direction. The variance has peaks when the buoys are aligned along the wave direction; angles  $0^\circ$ ,  $90^\circ$  and  $180^\circ$ , and also to a smaller extent at the  $45^\circ$  intervals. An optimal configu-

ration with high energy absorption and small power fluctuations would be at  $\pm 20^\circ$  and  $\pm 70^\circ$ .

## D. Sea states

Clearly, the sea state strongly affect the performance of individual WECs and wave energy parks. More energetic sea states will, generally speaking, result in larger power output. This is nothing new, and the power simulations plotted in figure 5-6 serve as a control test for this.

However, less is known of how the power fluctuations are affected by the sea state. The nine sea states investigated in figure 5-6 all display a more or less oscillatory pattern as a function of separating distance between units, with a clear dependence on the sea states. The sea states in figure 5, sharing the same energy period but different significant wave height, have similar oscillatory patterns, with peak variance at  $\sim 20$  m and local variance minimas at 10 m and  $\sim 35$  m. The sea states in figure 6, on the other hand, differ in the energy period but share the same significant wave height. Again, the variance is strongly affected of both the sea states and the separating distance between the devices. All wave climates studied in this paper share the property that local minimas and maximas for the power fluctuations (for square arrays of 9 WECs) occur at separating distances of 10-15 m and 20-35 m, respectively.

## E. Size of buoys

The simulations of the geometries in figure 2 are compared in figure 7. All arrays consist of 9 devices in square, regular geometries with separating distances 20 m between adjacent WECs. Geometry 1-3 contain buoys of radii  $R_1 = 1.5$  m,  $R_2 = 2.0$  m, and  $R_3 = 3.5$  m, respectively; geometry 4-9 all consist of three buoys of each size.

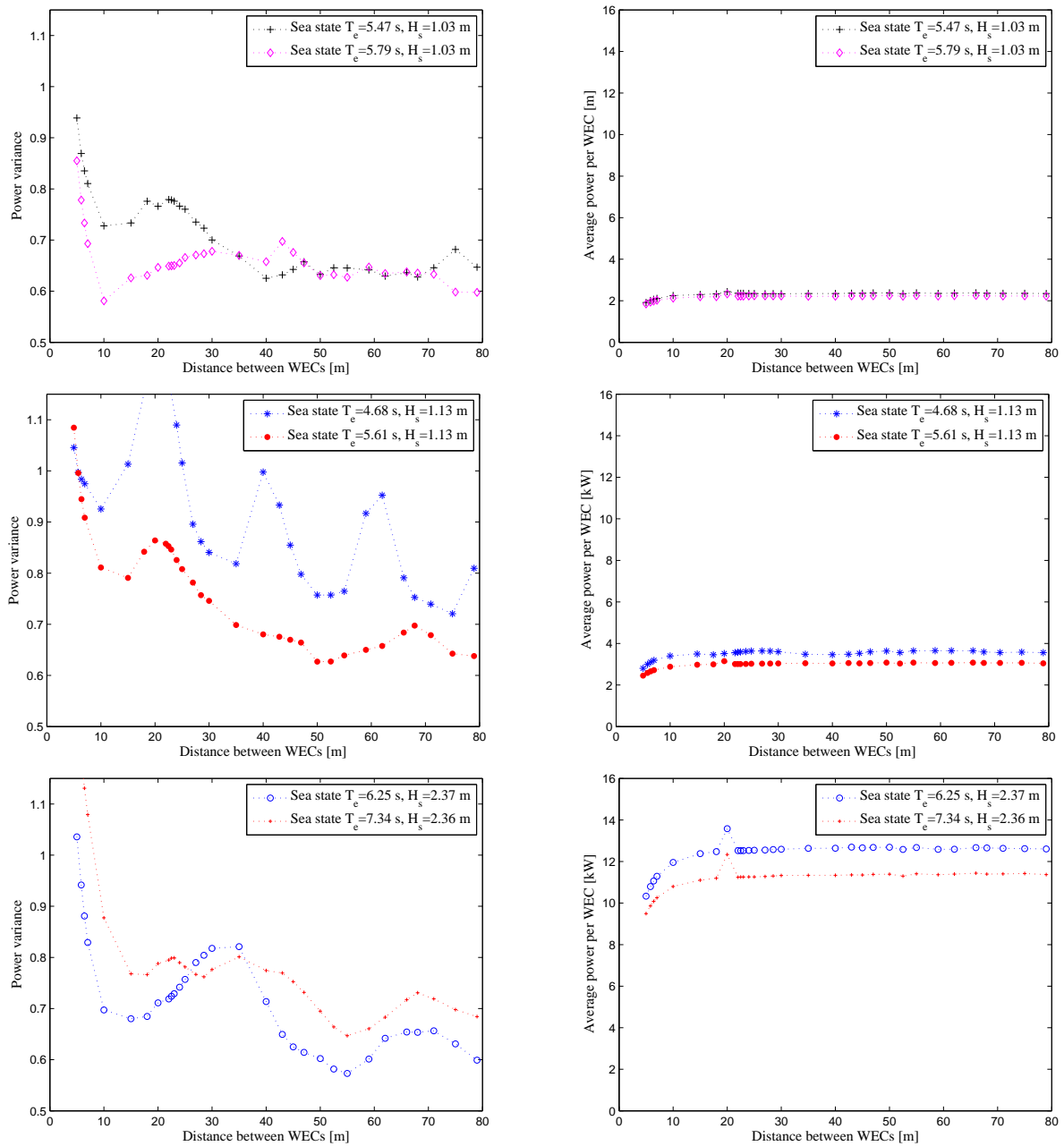


FIG. 6. Power variance and average power per buoy as functions of distance between adjacent devices in a wave energy park with 9 WECs. In each plots, two different sea states with comparable significant wave height but differing energy period are compared. The dotted lines are included only as a guidance for the eye.

As expected, the absorbed power increases with larger buoy size for geometry 1-3 (3.9 kW, 5.9 kW and 12.5 kW per WEC, respectively, in a park of 9 WECs). Based on these results, the expected power of an array consisting of three buoys of each size should be 67.1 kW. However, the absorbed power in geometries 4-9 differ from this value; geometry 6 has a lower energy absorption (59.0 kW), but geometry 4 has 14% higher energy absorption than the expected value. As we see, increasing the buoy size along the wave direction may increase the total power of the ar-

ray, and decreasing the buoy size along the wave direction may decrease the total power. The geometries 7-9 with the three different buoy sizes at random positions in the array (see figure 2) all have slightly higher power than the expected value. When comparing power fluctuations in geometries 4-9, geometry 6 with the largest buoys closest to the incoming wave stands out with significantly higher variance (1.29). Geometry 5, with increasing buoy radius perpendicular to the wave direction, has lowest variance in the group. The geometries 4-6 can be viewed as the

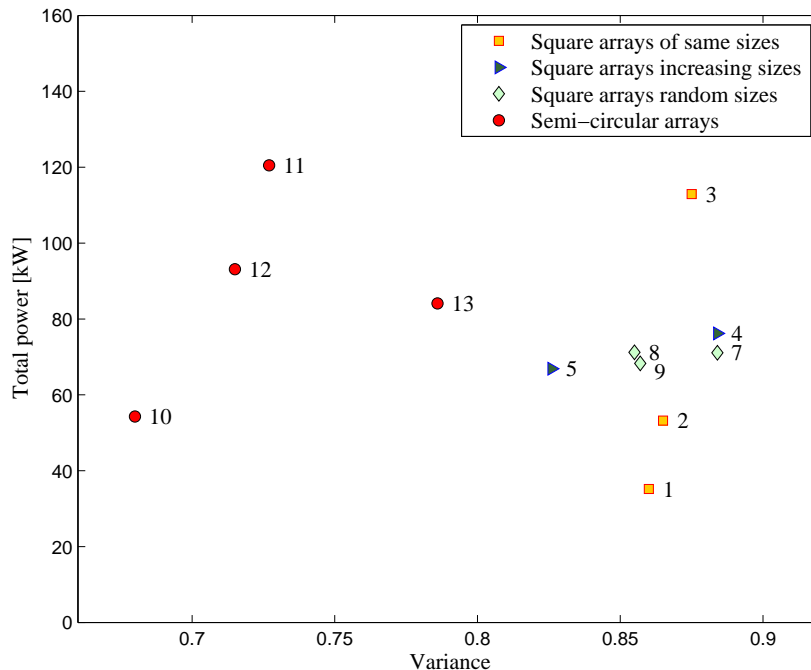


FIG. 7. Comparison of power variance and total power in geometries 1-13, depicted in figures 2-3. All geometries consist of 9 WECs and the incoming wave direction is along the x-axis. Geometry 6 has variance 1.29 and total power 59.0 kW and is not plotted in the figure. The sea state is characterized by energy period  $T_e = 5.01$  s and significant wave height  $H_s = 1.53$  m. Optimal configurations would have large power output and low variance, and hence end up in the upper left corner of this plot.

same array configuration with incoming wave angle  $0^\circ$ ,  $90^\circ$  and  $180^\circ$ , discussed in the context of varying wave directions above.

For the semi-circular geometries 10-13, the variance is again notably lower than for the rectangular ones. Based on the total power of geometry 10-11 with buoy radii  $R_2 = 2.0$  m and  $R_3 = 3.5$  m, respectively, the expected power for an array with five buoys of radius  $R_2$  and four of radius  $R_3$  would be 83.7 kW, and the converse case of four small and five large buoys would give an expected power of 91.1 kW. However, the output power of geometry 12 (with increasing buoy size along the wave direction) is 11% higher than the expected value, but the power of geometry 13 (with decreasing buoy size) is 8% less than the expected value. In addition, the fluctuations in geometry 12 are significantly lower than in geometry 13.

Note that the expected value for the power in this comparison was based on arrays with 9 WECs of the same type. If one instead would consider the interaction factor (3) discussed in section II, the expected power of isolated devices should be used. The isolated WECs of buoy radii 1.5 m, 2.0 m and 3.5 m have power output of 4.0 kW, 6.4 kW and 13.7 kW, respectively, which would correspond to a theoretical value of total power  $\sum P_j^{(\text{isolated})} = 72.3$  kW. From the total power of the geometry 4(-6) plotted in figure 8, one can deduce that the interaction factor is positive with  $Q > 1$  for incoming wave angles  $-55^\circ < \chi < 55^\circ$ , and destructive with  $Q < 1$  for remaining angles.

## V. DISCUSSION

Design of cost effective wave energy parks will necessarily involve the large challenge of how to reduce the power fluctuations, while simultaneously not substantially decreasing the power output or increasing costs or ocean area used. Many different parameters may affect the performance of individual devices and arrays of WECs, such as the global and local geometry of the array, the distance between units and the wave climate. In this paper, we study some of these parameters, with the overall aim to find guidelines for optimal configurations that enable low power fluctuations and high power output.

In section III B, some earlier results on the subject were reviewed. Whereas some of the earlier studies used a point-absorber assumption, others studied a few small configurations or performed experiments on a small number of buoys. The previous studies indicate that the fluctuations reduce with the number of interacting devices. Here, assuming full (linear) hydrodynamic interaction between all the units in the park, we show that the power variance as well as the power per WEC for a rectangular park are strictly decreasing functions of the number of buoys, as long as the separating distance between two adjacent units is kept constant, as discussed in section IV A. However, as seen in figure 4, adding more WECs to a park of constant area will not necessarily result in lowered fluctuations. This is due to the fact that the variance is also depending on the separating

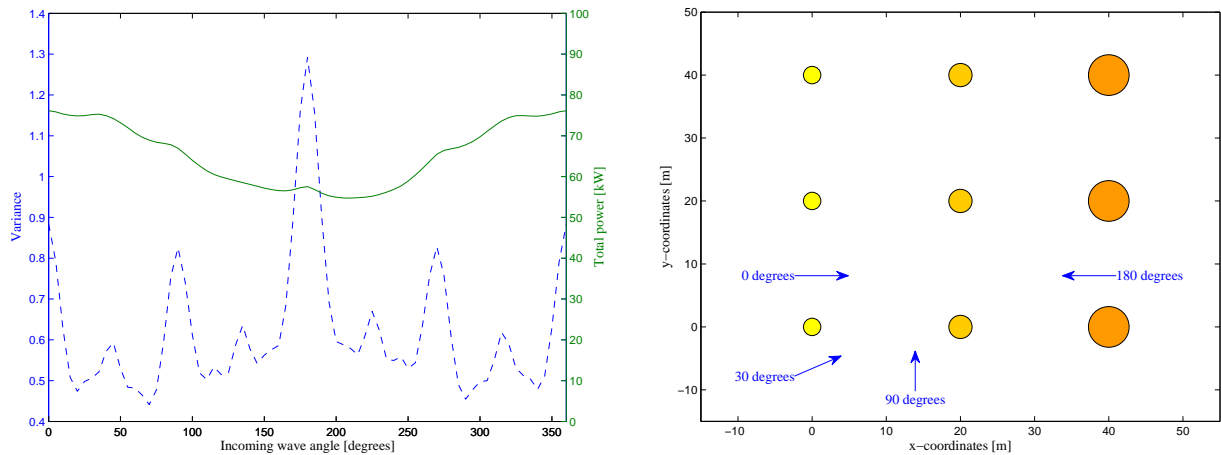


FIG. 8. a) Variance (dotted line) and total power (solid line) as a function of incoming wave angle. b) Park configuration and incoming wave directions.

distance between interacting units, as explored in more detail in section IV B and presented in figures 5-6. For a given sea state, the variance displays an oscillatory pattern as a function of the distance between devices. This pattern is more visible for some of the wave climates, which also shows that the magnitude of the fluctuations depend on the sea states. For all the sea states studied in this paper, minimum and maximum in the fluctuations are obtained at separation distance 10-15 m and 20-35 m, respectively. The average power per WEC is more or less constant for separating distances larger than 15 m. For the given WEC characteristics and array geometry, a separating distance of 10-15 m would mean a large gain in the lowered fluctuations, but only a small loss in the slightly lower power output.

The geometry of the array is another crucial factor for the performance of the wave energy park, as discussed in section IV C. In a previous paper, we found the variance to be reduced by three times for a semi-circular geometry with 32 WECs, as compared to a rectangular one<sup>9</sup>. In this study, semi-circular arrays have been included for comparison in figure 7. As before, we find that the semi-circular arrays have a less degree of power fluctuations; for arrays with 9 WECs about 80% of the rectangular ones. In realistic scenarios, the buoys will not be positioned on fixed grid lattice points, but will instead tend to drift slightly off their mean positions. In all the wave park configurations we have studied, this implies a slightly lowered power variance.

The incoming wave direction is an important parameter for the performance of a wave energy park. When optimizing wave park designs at a particular site, both the total power and the power fluctuations must be considered in relation to scatter diagrams of wave climates and the probability distribution of the wave direction at the specific location. The configurations optimal for high power production might not be the same ones that are optimal for lowering the fluctuations. As discussed in

section IV C, geometries where the devices are aligned along and perpendicular to the wave direction are non-favourable from the viewpoint of low variance. In figure 8, this corresponds to the cases where the incoming wave direction is a multiple of  $45^\circ$ . For the geometry 4(-6) in this paper, optimal configurations with high energy absorption and small power fluctuations correspond to incoming wave angles  $\pm 20^\circ$  and  $\pm 70^\circ$ . In addition, the interaction factor (3) is positive for incoming wave angles  $-55^\circ < \chi < 55^\circ$ .

In section IV E, arrays of buoys of different radii were studied and the results plotted in figure 7. Comparison of the rectangular geometries 1-9 reveal that mixing buoy sizes may give slightly higher total power, than the predicted value of three buoys of each size. Even more interesting is the comparison between semi-circular geometries 12 and 13, consisting of buoys of radius  $R_2 = 2.0$  m and  $R_3 = 3.5$  m in increasing and decreasing size along wave direction, respectively. As figure 7 shows, the former geometry has higher total power and significantly lower variance, despite the fact that it has only four buoys of the larger size, whereas the latter array has five.

To get an estimate of the relative influence of the parameters on the performance of a wave energy park, we perform a simple ANOVA statistical analysis between changing some of the parameters for a rectangular park. The results, pictured in figure 9, show that increasing the number of devices in a park is a more efficient way of reducing the power fluctuations (measured in terms of lowered power variance in percent) than randomizing the local geometry, and that aligning the array wisely relative to the common wave direction can be a very efficient way to reduce the fluctuations. The absorbed power decreases according to the same pattern, however. The result is statistically significant but should still be regarded only as an approximate guideline, since only a few array geometries have been compared.

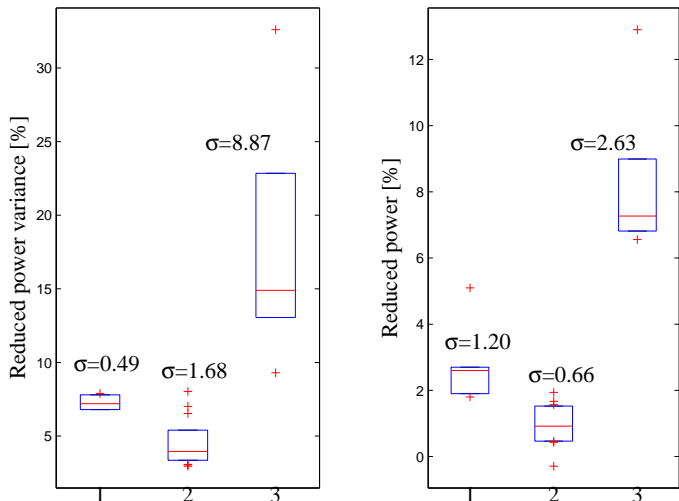


FIG. 9. Comparison of the relative influence of three actions performed on rectangular parks. The central mark is the median, the edges of the box are the 25th and 75th percentiles,  $\sigma$  is the standard deviation from the mean value, and the outliers are plotted individually.

1. *Increase number of WECs by 25-33%*: variance decreases by 7.3% and power by 2.8% (mean over the 6 data points in figure 4 where the no. of WECs increases by 25-33%).
2. *Randomizing local geometry*: variance decreases by 4.5% and power by 1.0% (mean over the 12 data points in fig. 4).
3. *Rotating  $90^\circ$  relative to wave direction*: the variance is decreased by 18% and the power by 8.3% (mean over the 5 data points in table II).

## VI. SUMMARY

For the design of economically viable and effective wave energy parks, all parameters affecting the power fluctuations and the total output power must be considered carefully. Simulations such as the ones in this paper can provide guidelines for optimal parameter values. Based on the discussion above, a few rules of thumb may be stated for the optimal design of wave energy parks:

- Increasing the number of WECs by around 30% may reduce the power fluctuations by roughly 7% and the average power by 3%. This can be cost effective for small arrays, but not for large parks.
- Changing the global geometry from rectangular (and perpendicular with the wave direction) to semi-circular may reduce the power fluctuations as much as 20%, and also improve the average power absorption by a few percent.
- Positioning the WECs on slightly randomized positions instead on fixed grid points may reduce the variance by around 4.5% but also the power by 1%.
- Using WECs with increasing buoy radius along the wave direction may increase power absorption by

10-15%. Similarly, decreasing buoy radius along the wave direction could lower the power by 10%.

- Analysing the predominant wave directions at a site and positioning the array accordingly may improve both magnitude and quality of the power delivered. As an example, the array in figure 8 has a constructive interaction ( $Q > 1$ ) and lower average variance (0.59) for wave angles  $\chi \in [-55^\circ, 55^\circ]$ , but destructive interaction and higher average variance (0.64) for angles outside this range.

## ACKNOWLEDGMENTS

This project is supported by StandUp for Energy, Upsala University, Carl Tryggers Stiftelse, the Swedish Energy Agency, Bengt Ingeströms scholarship fund and the Wallenius foundation. M.G. would in particular like to thank Dr. Jochem Weber, NUI Maynooth, Ireland, for the discussion arrays with buoys of different radii.

- <sup>1</sup>R. Shaw. *Wave Energy – A Design Challenge*. Ellis Horwood Ltd, Chichester, UK, 1982.
- <sup>2</sup>S.H. Salter. World progress in wave energy - 1988. *The Int. Journal of Ambient Energy*, 10:3–24, 1989.
- <sup>3</sup>K. Thorburn and M. Leijon. Farm size comparison with analytical model of linear generator wave energy converters. *Ocean Engineering*, 34(5-6):908–916, 2007.
- <sup>4</sup>J. Tissandier, A. Babarit, and A. Clement. Study of the smoothing effect on the power production in an array of searev wave energy converters. In *The 18th Int. Offshore and Polar Engineering Conference, Vancouver, Canada*, July 2008.
- <sup>5</sup>M. Rahm, O. Svensson, C. Boström, R. Waters, and M. Leijon. Experimental results from the operation of aggregated wave energy converters. *Renewable Power Generation, IET*, 6(3):149–160, 2012.
- <sup>6</sup>J. Sjolte, G. Tjensvoll, and M. Molinas. Power collection from wave energy farms. *Appl. Sci.*, 3:420–436, 2013.
- <sup>7</sup>M. Vicente, M. Alves, and A. Sarmiento. Layout optimization of wave energy point absorbers arrays. In *Proc. of the 10th EWTEC, Aalborg, Denmark*, Sept. 2013.
- <sup>8</sup>A. Babarit. On the park effect in arrays of oscillating wave energy converters. *Renewable Energy*, 58:68–78, 2013.
- <sup>9</sup>J. Engström, M. Eriksson, M. Göteman, J. Isberg, and M. Leijon. Performance of a large array of point-absorbing direct-driven wave energy converters. *J. Applied Physics*, 114:204502, 2013.
- <sup>10</sup>K. Budal. Theory for absorption of wave power by a system of interacting bodies. *Journal of Ship Research*, 21:248–253, 1977.
- <sup>11</sup>G. Thomas and D.V. Evans. Arrays of three dimensional wave energy absorbers. *Journal of fluid mechanics*, 108:67–88, 1981.
- <sup>12</sup>C. Fitzgerald and G. Thomas. A preliminary study on the optimal formation of an array of wave power devices. In *Proc. of the 7th EWTEC, Porto, Portugal*, Sept. 2007.
- <sup>13</sup>H. Wolgamot, R. Eatock Taylor, P.H. Taylor, and C.J. Fitzgerald. The interaction factor for wave power in arrays. In *Proc. of the 26th IWWWFB, Athens, Greece*, April 2011.
- <sup>14</sup>M. Leijon, R. Waters, M. Rahm, O. Svensson, C. Boström, E. Strömstedt, J. Engström, S. Tyrberg, A. Savin, H. Gravråkmö, H. Bernhoff, J. Sundberg, J. Isberg, O. Ågren, O. Danielsson, M. Eriksson, E. Leijerskog, B. Bolund, S. Gustafsson, and K. Thorburn. Catch the wave to electricity: The conversion of wave motion to electricity using a grid-oriented approach. *IEEE Power & Energy Magazine*, 7(1):50–54, 2009.
- <sup>15</sup>R. Waters, J. Engström, J. Isberg, and M. Leijon. Wave climate off the Swedish west coast. *Renewable Energy*, 34(6):1600, 2009.

- <sup>16</sup>M. Folley and T.J.T. Whittaker. The effect of sub-optimal control on the spectral wave climate on the performance of wave energy converter arrays. *Applied Ocean Research*, 31:260–266, 2009.
- <sup>17</sup>B.F.M. Child and P. Laporte Weywada. Verification and validation of a wave farm planning tool. In *Proc. of the 10th EWTEC, Aalborg, Denmark*, Sept. 2013.
- <sup>18</sup>P. Ricci, J.B. Saulnier, and A.F. de Falcão. Point-absorber arrays: a configuration study off the portuguese west-coast. In *Proc. of the 7th EWTEC, Porto, Portugal*, Sept. 2007.
- <sup>19</sup>B. Borgarino, A. Babarit, and P. Ferrant. Impact of wave interactions effects on energy absorption in large arrays of wave energy converters. *Ocean Engineering*, 41:79–88, 2012.
- <sup>20</sup>B.F.M. Child, J. Cruz, and M. Livingstone. Development of a tool for optimising arrays of wave energy converters. In *Proc. of the 9th EWTEC, Southampton, UK*, Sept. 2011.
- <sup>21</sup>J. Sjolte, B. Sorby, G. Tjensvoll, and M. Molinas. Annual energy and power quality from an all-electric wave energy converter array. In *15th Int. Power Electronics and Motion Control Conference, Novi Sad, Serbia*, 2012.
- <sup>22</sup>J. Sjolte, G. Tjensvoll, and M. Molinas. All-electric wave energy converter connected in array with common dc-link for improved power quality. In *Proc. of the 3rd IEEE International Symposium on Power Electronics for Distributed Generation Systems (PEDG), Aalborg, Denmark*, June 2012.